Smart Organic/Inorganic Hybrid Nanoobjects with Controlled Shapes by Self-Assembly of Gelable Block Copolymers

Ke Zhang, Lei Gao, and Yongming Chen*

State Key Laboratory of Polymer Physics and Chemistry, Joint Laboratory of Polymer Sciences and Materials, Institute of Chemistry, The Chinese Academy of Sciences, Beijing 100080, P. R. China

Received September 27, 2007; Revised Manuscript Received January 9, 2008

ABSTRACT: A series of well-defined functional gelable diblock copolymers, poly(3-(triethoxysilyl)propyl methacrylate)-*block*-poly(2-vinylpyridine) (PTEPM-*b*-P2VP), were synthesized by a two-step reversible addition−fragmentation chain transfer (RAFT) mediated radical polymerization procedure. The self-assembly of PTEPM-*b*-P2VP diblock copolymers in the bulk was studied by a combination of small-angle X-ray scattering (SAXS) and transmission electron microscopy (TEM). With change of the copolymer composition, three different microphase-separated morphologies, i.e., lamellae, hexagonally packed cylinders, and spheres, were obtained. The in-situ self-gelation was subsequently carried out under hydrochloric acid vapor to lock the PTEPM phases. By dispersing the gelated bulk materials with ordered structures in an acidic water solution (pH = 3), the isolated organic/inorganic hybrid nanoobjects with controlled shapes including plates, cylinders, and spheres bearing protonated P2VP hairs were prepared. By deprotonation of the P2VP hairs, these novel nanoobjects may precipitate from the solution, and therefore, they are pH-sensitive. Furthermore, when applying these hybrid nanoobjects with P2VP hairs as the templates for supporting gold nanoparticles, novel pH-responsive functional nanoobjects with Au nanoparticles organized in different dimension were obtained.

Introduction

Block copolymers may microphase separate in bulk into a series of well-defined nanoscopic morphologies simply by changing their molecular parameters.[1−3] During the past decade, these organic ordered structures have been widely used in nanotechnologies, such as preparation of nanoobjects,[4] nanocomposites,[5,6] photonic band gap materials,[7] and lithographic templates,[8,9] etc. By cross-linking one domain of the preformed nanostructures from block copolymers in bulk and dispersing them in a good solvent for the un-cross-linked domain, a range of nanomaterials with controlled shape, size, and compositions are easily produced. These nanomaterials may find considerable applications in areas related with drug delivery, catalysis, photonics, energy generation and storage, electronics, etc.

Two main approaches have been developed in this field. One is to directly fix the specific domains of the preformed assembly based on the block copolymers with a cross-linkable functional block, which mostly produces pure organic nanomaterials.[10−21] The other is to use the block copolymers as structure-directing agents for the metal oxide precursors to prepare organic/inorganic nanohybrids, where the suitable block copolymers were limited strictly.[4,22−27] By the latter approach, dispersible individual nanoobjects may also be prepared. In this case, the inorganic components are enriched in one polymer domain, and therefore, the block copolymers are actually trapped into the inorganic rich domains by physical interaction. Recently, we have combined the merits of these two methods to obtain organic/inorganic hybrid plates, cylinders, and spheres by using microphase separation of the gelable block copolymers, poly(3-(triethoxysilyl)propyl methacrylate)-*block*-polystyrene.[28] The advantage of the present approach is that the inorganic precursor segments are linked with the block copolymers covalently. Therefore, controlling the morphology of hybrid nanoobjects using block copolymer self-assembly becomes much more versatile.

It will be important to functionalize thus produced block copolymer materials with nanostructure. Until now, there are only few reports about preparing functional nanoobjects based on the above method. Liu et al. used poly(*tert*-butyl acrylate)-*block*-poly(2-cinnamoylethyl methacrylate) to prepare thin films with regularly packed channels bearing functional poly(acrylic acid) (PAA) hairs inside, whose permeability of water can be tuned by pH or cation type.[20] These porous films have also been used as templates to load CdS or Fe_2O_3 nanopartices inside the functional nanochannels.[21] Similarly, they also used polystyrene-*block*-poly(2-cinnamoyloxyethyl methacrylate)-*block*-poly(*tert*-butyl acrylate) to prepare isolated superparamagnetic nanotubes, where Fe_2O_3 nanoparticles were impregnated inside the nanocavities.[18] Wiesner et al. have used an amphiphilic diblock copolymer, poly(isoprene-*block*-ethylene oxide) (PI-*b*-PEO), as a structure-directing agent to prepare magnetic silica-type nanoparticles with different shapes.[25] When changing the composition of PI-*b*-PEO and the fraction between block copolymers and metal alkoxides, they have obtained mesporous aluminosilicate materials with superparamagnetic Fe_2O_3 particles embedded in the walls.[26]

However, as far as we knew, there is no report to prepare stimulus responsive hybrid nanoobjects based block copolymer self-assembly in bulk. If the polymer hairs bearing on the surface of the isolated nanoobjects are responsive to pH stimulus, novel "smart" block copolymer nanoobjects with controlled shapes and compositions can be obtained easily. Furthermore, if the hairs are functional polymers, inorganic nanoparticles can also be produced inside the hairs. These nanoobjects may have important potential application for example as supports of catalysts, medicine, and diagnostic agents.

As an extension of previous work of this group,[28] herein, we report the microphase separation behaviors of a novel class of gelable block copolymer, poly(3-(triethoxysilyl)propyl methacrylate)-*block*-poly(2-vinylpyridine) (PTEPM-*b*-P2VP), which

* Corresponding author: phone +0086-10-62659906; Fax +0086-10-62559373; e-mail ymchen@iccas.ac.cn.

10.1021/ma7021698 CCC: $40.75
Published on Web 02/16/2008

Scheme 1. Preparation of P2VP Functionalized Organic/Inorganic Hybrid Nanoobjects with Different Morphologies and Organization of Gold Nanoparticles along Surfaces of the Hybrids[a]

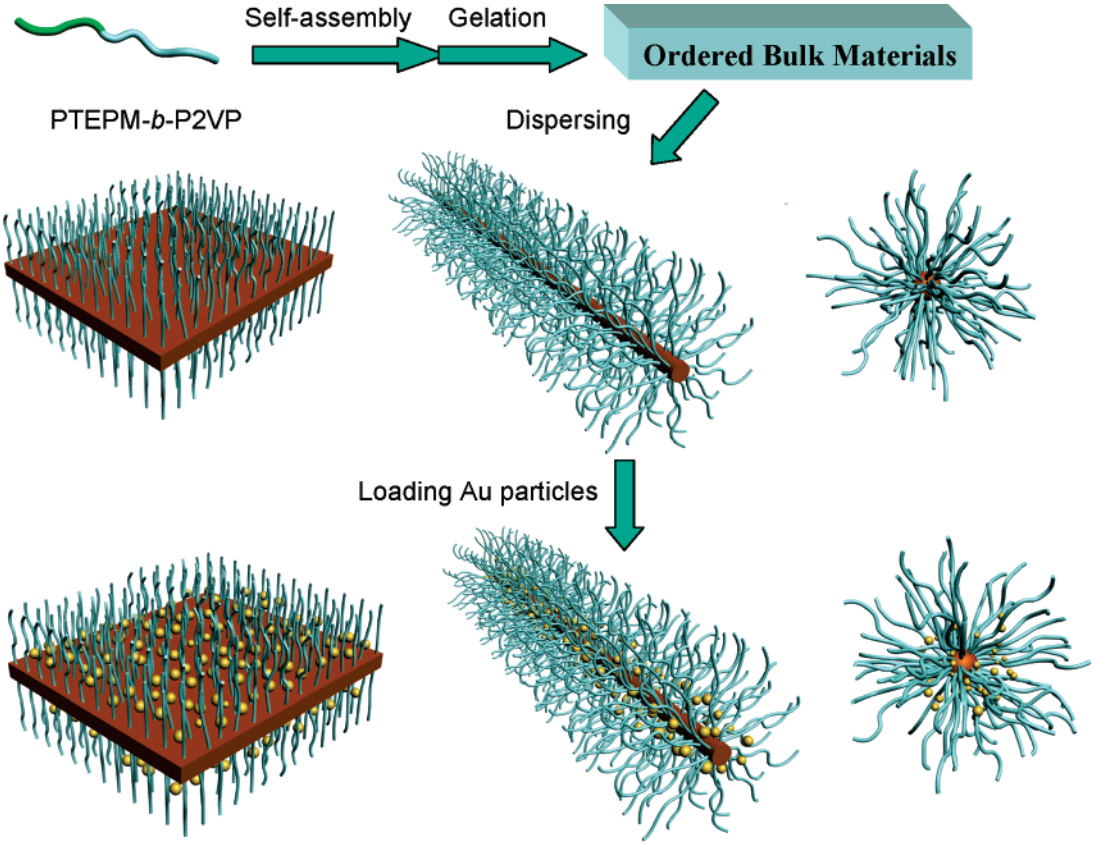

[a] Light blue coil: P2VP; green coil: ungelated PTEPM; brown plate, cylinder, and sphere: gelated PTEPM domains; yellow spheres: gold nanoparticles.

were synthesized by RAFT mediated radical polymerization. As presented by Scheme 1, after an in-situ self-gelation procedure of PTEPM domains in the preformed ordered bulk materials, a series of novel water-soluble isolated organic/inorganic hybrid nanoobjects with controlled shapes bearing poly(2-vinylpyridine) (P2VP) hairs have been obtained by dissolving the gelated bulk materials into acid water solution. It is known that P2VP is a very important functional polymer, which can be used to make pH-sensitive materials and provides potential supramolecular interactions such as hydrogen bonding and metal coordination.[29] So, present novel hybrid nanoobjects of different morphologies bearing P2VP hairs not only show pH-responsive character but also are used to align metal nanoparticles in different dimension.

Experimental Section

Materials. 2-Vinylpyridine (97%, Aldrich) was dried over calcium hydride overnight and distilled under a reduced pressure. 3-(Trimethoxysilyl)propyl methacrylate (>95%, Wuhan University Silicone New Material Co.) was used as received. 3-(Triethoxysilyl)propyl methacrylate (TEPM) was synthesized according to a literature from 3-(trimethoxysilyl)propyl methacrylate.[30] 2-Cyanoprop-2-yl dithiobenzoate (CPDB) was synthesized according to the literature.[31] 2,2-Azoisobutyronitrile (AIBN) was recrystallized from methanol and stored at 4 °C. Anhydrous ethanol (>99%, Beijing Chemical Reagent Co.) was refluxed over magnesium. Anhydrous methanol, tetrahydrofuran (THF), toluene, benzene (>99%, Beijing Chemical Reagent Co.), and other chemicals were used as received.

Synthesis of PTEPM Macromolecular Chain Transfer Agent (Macro-CTA). Bulk polymerization of TEPM was performed in a sealed ampule equipped with a stir bar under vacuum. A typical procedure was as follows: CPDB (121.4 mg, 5.48×10^{-1} mmol), TEPM (10.4 g, 35.8 mmol), and AIBN (9.0 mg, 5.48×10^{-2} mmol) were added into a 30 mL glass ampule. The mixture was degassed through four freeze−evacuate−thaw cycles, and then the ampule was sealed under vacuum. The polymerization was carried out in an oil bath at 60 °C for 20 h. The reaction was terminated by cooling reaction the mixture with an ice bath. The resulted crude product was purified by precipitating into a large amount of methanol and water mixture (7:3 volume ratio) three times. Monomer conversion was determined by the ^{1}H NMR spectrum.

Synthesis of PTEPM-*b*-P2VP Diblock Copolymer. The polymerization was performed in a sealed ampule equipped with a stir bar under vacuum. A general procedure: PTEPM macro-CTA (2.80 g, $M_{n,NMR} = 17\,300$; $M_w/M_n = 1.10$), 2-vinylpyridine (23.30 g, 219.5 mmol), and AIBN (3.0 mg, 1.83×10^{-2} mmol) were charged into a 50 mL Schlenk flask. The mixture was degassed by four freeze−evacuate−thaw cycles and then flame-sealed under vacuum. Polymerization was carried out in an oil bath thermostated at 60 °C for 13 h. The reaction was terminated by cooling and exposing the mixture to air. The resulting product dissolved in ethanol was purified by precipitating into hexane three times. The composition was determined by the ^{1}H NMR spectrum.

Bulk Casting and Annealing of PTEPM-*b*-P2VP. The casting and annealing of all PTEPM-*b*-P2VP diblock copolymers into bulk samples were carried out analogously and a representative procedure was described. A solution of PTEPM-*b*-P2VP diblock copolymer (50 mg/mL) in THF was spread onto a clean Teflon plate, and the solvent was allowed to evaporate in a vacuum desiccator over 5 days. The resulting bulk sample (ca. 0.5 mm in thickness) was then dried for 12 h under vacuum at 60 °C. Thermal annealing was conducted at 115 °C for 24 h under argon to give the block copolymer bulk sample with microphase separation.

Self-Gelation in Microdomain Structure and Preparation of Nanoobjects. The PTEPM-*b*-P2VP bulk samples with microphase separation structure were exposed to HCl acid atmosphere for about

Scheme 2. Synthesis of PTEPM and Its Block Copolymer of P2VP by RAFT Mediated Radical Polymerization

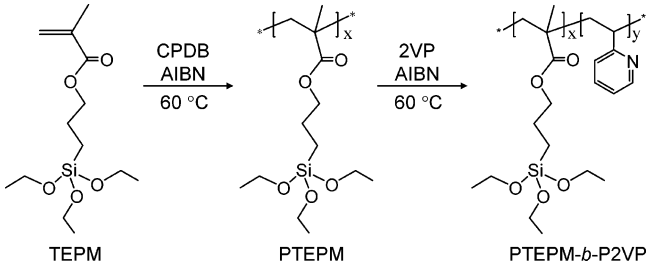

1 h and then dried under vacuum at temperature of 60 °C for 12 h to carry out the sol−gel reaction of the PTEPM domain for completion. After cross-linking, the samples were immersed in HCl water solution (pH = 3) and stirred. The films disappeared and a colloid solution was obtained in around 1 day.

Preparation of Nanoobjects Loaded with Gold Nanoparticles. After dispersing the gelated hybrid bulk materials (5 mg) in HCl water solution (pH = 3) (2 mL) and stirred for 3 days, a water solution of $NaAuCl_4$ (ca. 1 mg/mL) was added slowly, where the molar ratio between 2VP and $NaAuCl_4$ was fixed to 1:0.2. After the mixture solution was stirred for ca. 24 h, a freshly prepared aqueous solution of sodium borohydride (10 mg/mL) (ca. 0.1 mL) was added dropwise, and the solution was stirred for about 10 h.

Characterization. Gel permeation chromatography (GPC) was performed by a set of a Hitachi L-2130 pump, a Waters 2410 refractive index detector, and a Waters 2487 ultraviolet detector, the combination of Hersteller MZ-Gel SDplus 5 μm, porosity 10^3, 10^4, 10^5, and 10^6 Å. THF was used as eluent at flow rate of 1.0 mL/min at 40 °C. Polystyrene standards were used for the calibration. GPC analysis was also performed by a set of a Hitachi/Merck L-7100 pump, a Waters 2414 refractive index detector, and a Waters 486 ultraviolet detector, the combination of Hersteller MZ-Gel SDplus 5 μm, porosity 100, 10^3, 10^4, and 10^6 Å. DMF with 1 g/L LiBr was used as eluent at flow rate of 1.0 mL/min at 60 °C. Polystyrene standards were used for the calibration.

^{1}H NMR spectra were recorded on a Bruker DMX400 spectrometer with $CDCl_3$ as solvent at room temperature.

Fourier-transform infrared (FT-IR) spectroscopy was recorded by a deuterated triglycine sulfate (DTGS) detector on a Bruker EQUINOX 55 spectrometer and processed by the Bruker OPUS program. Samples were prepared by milled with potassium bromide (KBr) to form a very fine powder and then compressed into a thin pellet.

Transmission electron microscopy (TEM) images were obtained using a Hitachi H-800 instrument operated at an accelerating voltage of 100 kV. The images were recorded by a digital camera. Bulk samples were embedded in epoxy and cured at 40 °C overnight. Thin sections (50−100 nm) were obtained using Leica Ultracut UCT ultramicrotome and a diamond knife at room temperature. The microtomed sections were stained by I_2 vapor 30 min before observation. Solution samples were dropped onto carbon-coated copper grids for TEM observation.

SAXS experiments were performed on a SAXS system in Max-Planck-Institute for Polymer Research in Mainz. The system is composed of a two-dimensional detector (Bruker Histar), a mirror (Osmic), and a rotating anode X-ray generator (Rigaku Mikro max 007) operated at 30 kV and 10 mA. The wavelength of the incident X-ray beam from Cu Kα radiation is $\lambda = 0.154$ nm.

Results and Discussion

1. Synthesis and Characterization of PTEPM-*b*-P2VP Diblock Copolymers. PTEPM-*b*-P2VP diblock copolymers were synthesized by a two-step RAFT procedure (Scheme 2), in which the first PTEPM block was isolated after the polymerization and then was used as a macro-CTA for synthesizing the second block of P2VP.

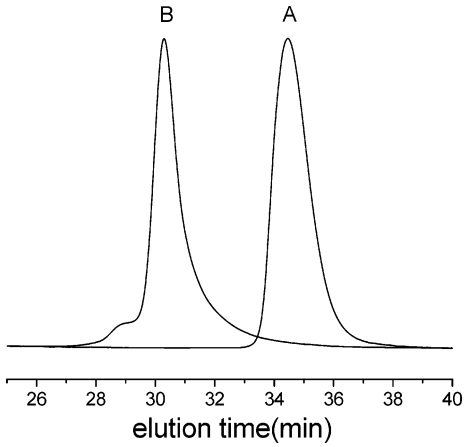

Figure 1. GPC curves (RI) of (A) a PTEPM macro-CTA, sample 3 in Table 1, and (B) the corresponding $PTEPM_{58}$-*b*-$P2VP_{474}$ diblock copolymer, sample 4 in Table 1. DMF with 1 g/L LiBr used as the eluent.

Polymerization of TEPM was performed in bulk using CPDB as a RAFT agent and AIBN as an initiator. The molar ratio between CPDB and AIBN was fixed to 10/1. After degassed by freeze−evacuate−thaw cycles, the sealed ampule with mixture was thermostated to 60 °C. Monomer conversion and actual molecular weight were determined by the ^{1}H NMR spectrum as demonstrated in previous report.[28] Shown in Figure 1A is the GPC curve of PTEPM homopolymer (run 3 in Table 1) in DMF, indicating a monomodal peak.

The PTEPM homopolymer was then used as a macro-CTA to synthesize PTEPM-*b*-P2VP diblock copolymers, where AIBN was used as initiator. The molar ratio between macro-CTA and AIBN was also fixed to 10/1. After degassing, the sealed ampule with mixtures was thermostated to 60 °C. Figure 1B is the GPC curve of PTEPM-*b*-P2VP diblock copolymer (run 4 in Table 1) in DMF using standard polystyrenes as a calibration. Compared with its macro-CTA (Figure 1A), a peak with a polydispersity of 1.18 at the higher molecular weight direction was displayed, and no peak of the residual macro-CTA was observed, indicating the successful polymerization of diblock copolymer. Furthermore, a very small shoulder peak with a molecular weight twice than that of the main peak was also observed, which may be caused by the coupling reactions of propagating radicals. Because the GPC was calibrated with polystyrene standards, the absolute number molecular weights and composition of diblock copolymers were obtained from the ^{1}H NMR analysis. A representative ^{1}H NMR spectrum of PTEPM-*b*-P2VP and the peak assignments are shown in Figure 2, from which the composition can be calculated by comparing the peak areas of the protons derived from two blocks, e.g., m (*H* adjacent to N of 2VP) in P2VP block and e ($-CH_2Si$) in PTEPM block.

The diblock copolymers with different lengths of PTEPM and P2VP segments were thus synthesized by changing the macro-CTA and the feed ratios of TEPM to macro-CTA. As a result, three diblock copolymers were prepared, and their properties are summarized in Table 1.

2. Self-Assembly of PTEPM-*b*-P2VP Diblock Copolymers in the Bulk State. To study the morphologies of microphase separation in bulk state, three polymers with different compositions (runs 4−6 in Table 1), $PTEPM_{58}$-*b*-$P2VP_{474}$, $PTEPM_{37}$-*b*-$P2VP_{540}$, and $PTEPM_{35}$-*b*-$P2VP_{1360}$, were selected as representative examples. The bulk materials of three block copolymers were characterized by a combination of small-angle X-ray scattering (SAXS) and transmission electron microscopy (TEM).

Table 1. Radical Polymerizations of the PTEPM Mediated by CPDB and Properties of PTEPM-*b*-P2VP

run[a]	feed ratio[b]	conv (%)[c]	$M_{n,NMR}$	$M_{n,GPC}$	M_w/M_n	TEPM/2VP[c]	W_{PTEPM} (%)	structure[d]
1	45:1	77.8	10 200	9 400	1.08	35/0		
2	45:1	82.5	11 100	10 500	1.15	37/0		
3	65:1	89.9	17 300	15 600	1.10	58/0		
4	1200:1	39.5	67 600	75 800	1.18	58/474	25.6	lam
5	1800:1	30.0	68 100	87 200	1.15	37/540	16.3	hex
6	3000:1	45.3	155 000	184 000	1.26	35/1360	6.6	sphere

[a] Runs 1−3 show the PTEPM homopolymers. Their $M_{n,GPC}$ and M_w/M_n were obtained by GPC with THF as eluent. Runs 4−6 show the synthesis and characteristics of the PTEPM-*b*-P2VP diblock copolymers. Their $M_{n,GPC}$ and M_w/M_n were obtained by GPC with DMF as eluent. [b] TEPM/CPDB (molar ratio) for runs 1−3, 2VP/macro-CTA (molar ratio) for runs 4−6. [c] Calculated by the ^{1}H NMR spectrum. [d] Microphase separation morphology: lam means alternating PTEPM and P2VP lamellae; hex means hexagonally packed PTEPM cylinders in P2VP matrix; sphere means PTEPM spheres in P2VP matrix.

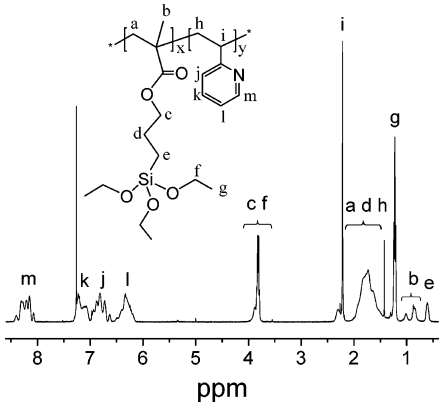

Figure 2. ^{1}H NMR spectra of $PTEPM_{58}$-*b*-$P2VP_{474}$ diblock copolymer in $CDCl_3$, sample 4 in Table 1.

For TEM analysis, all ultramicrotomed slices embedded in epoxy resin were stained with I_2 vapor to dye the P2VP microdomains; therefore, the dark areas in the TEM images correspond to P2VP domains. The SAXS curves and TEM photographs of the microphase structure are shown in Figure 3. For polymer $PTEPM_{58}$-*b*-$P2VP_{474}$, whose molecular weight fraction of PTEPM block was 25.6%, a highly ordered lamellar morphology was obtained. As shown in Figure 3A (left), the SAXS curve gave six different peaks with a peak position pattern of 1:2:3:4:5:6, consistent with a lamellar morphology. From the primary peak position value at low q, the average domain spacing was calculated to be 45.1 nm. Demonstrated in Figure 3A (right) was the corresponding TEM photograph of a microtomed slice, in which an ordered array of alternating PTEPM and P2VP lamellae was observed and the dark layer was the stained P2VP microdomain. The average domain spacing measured from TEM photograph was 48 nm, which was similar to the data obtained from SAXS curve.

For polymer $PTEPM_{37}$-*b*-$P2VP_{540}$, a diblock copolymer with a weight fraction of PTEPM block of 16.3%, a highly ordered cylindrical morphology was formed. As demonstrated in the SAXS curve in Figure 3B (left), the peaks with position ratio of a ratio $1:\sqrt{3}:\sqrt{7}$ supported a hexagonally packed cylinder morphology. From the value of main peak position, the average periodicity was calculated to be 36.1 nm. Shown in Figure 3B (right) is the TEM photograph of a microtomed slice. An ordered array of PTEPM cylinders in the P2VP matrix with an average periodicity of 38 nm was displayed.

As for the polymer $PTEPM_{35}$-*b*-$P2VP_{1360}$, whose molecular weight fraction of PTEPM block was 6.6%, the microphase separation produced a disordered spherical morphology. Figure 3C (left) is the SAXS curve of this sample, whose features are consistent with a liquidlike packing of spheres. As revealed in Figure 3C (right), the TEM photograph of a microtomed slice displayed a disordered array of PTEPM spheres in the P2VP matrix.

3. Preparation of pH-Responsive Organic/Inorganic Hybrid Nanoobjects. After the microphase separation of diblock copolymers, the dispersed PTEPM phases were distributed in the P2VP phases as lamellae, cylinders, and spheres. The PTEPM-*b*-P2VP diblock copolymers contained a gelable PTEPM block, which may be used to conduct sol−gel reaction under acid or basic conditions. To carry out the gelation reaction of the PTEPM block, the materials having tailored microphase structures were exposed to a hydrochloric acid atmosphere for about 1 h and then treated by a calcination process at 60 °C under vacuum. IR results shown in Figures S1A (before cross-linking) and S1B (after cross-linked) (Supporting Information) proved that the cross-linking reaction completed under this condition.[28] At this stage, the PTEMP phases of above three structures were transformed into silica oxide networks confined in the preformed microdomains. As shown in a recent report,[28] this self-gelation process did not alter the preformed morphologies of poly(3-(triethoxysilyl)propyl methacrylate)-*block*-polystyrene. To further prove this for present system, a comparison of SAXS results of lamellar morphology formed by a different polymer $PTEPM_{60}$-*b*-$P2VP_{162}$ before and after cross-linking the PTEPM domains was supplied as shown in Figure S2 (in Supporting Information). We noticed that the periodic length shrank from 32.4 to 30.4 nm due to the cross-linking of the PTEPM microdomains, but the lamellar morphology was not changed. When the sol−gel reaction in PTEPM microphase is completed, these gelated materials may be dispersed in the solvent of P2VP matrix. Well-defined nanoobjects bearing P2VP hairs with different shapes can be obtained according to the microphase separation morphologies.

P2VP may dissolve in the acidic water since the pyridine units may be protonated; however, it may precipitate in basic water. Therefore, P2VP is a pH-responsive polymer, which allows us to prepare a novel kind of organic/inorganic hybrid nanoobjects with pH-responsive character. To prepare these hybrid nanoobjects, the hybrid bulk materials were dispersed in a water solution of hydrochloric acid (pH = 3) for about 3 days with stirring. The macroscopic materials disappeared, and the appearances of the dispersed nanoobjects are shown in Figure 4 (left column). For the sample of $PTEPM_{58}$-*b*-$P2VP_{474}$, the solution looked translucent (Figure 4A (left)), indicating the large size of dispersion. For the sample of $PTEPM_{37}$-*b*-$P2VP_{540}$, the solution became transparent, and a blue tint implied the dispersion with small and uniform size (Figure 4B (left)). When the sample of $PTEPM_{35}$-*b*-$P2VP_{1360}$ was dispersed, the solution became clearer (Figure 4C (left)). Shown in Figure 4 (right column) are the TEM images of the obtained hybrid nanoobjects with different shapes. Dispersing the lamellar hybrid materials of $PTEPM_{58}$-*b*-$P2VP_{474}$, isolated organic/inorganic hybrid plates with a uniform thickness were obtained (Figure 4A (right)).

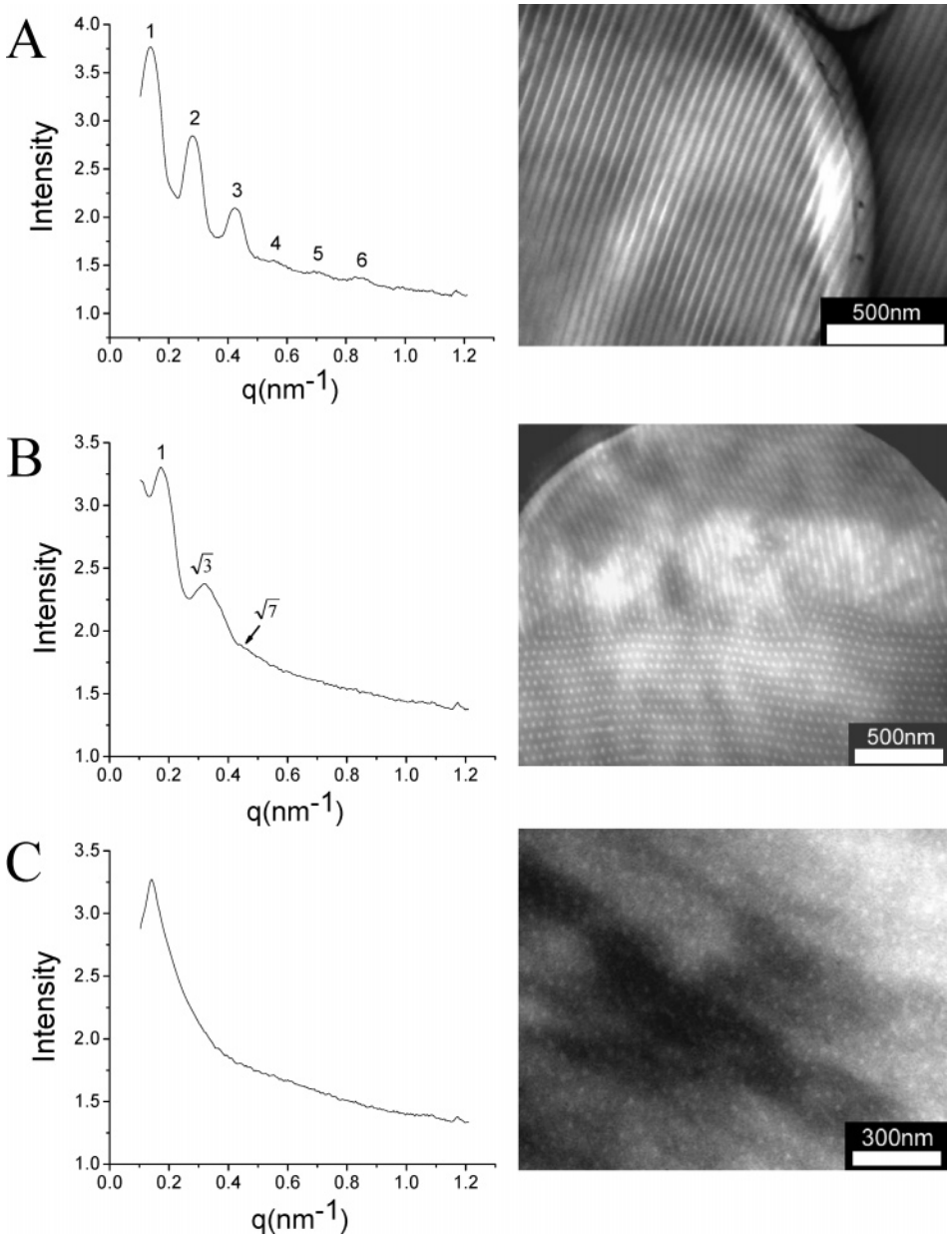

Figure 3. Small-angle X-ray scattering curves (shown on left) and TEM images of microtomed silices (shown on right) of the bulk samples from (A) $PTEPM_{58}$-*b*-$P2VP_{474}$ (B) $PTEPM_{37}$-*b*-$P2VP_{540}$, and (C) $PTEPM_{35}$-*b*-$P2VP_{1360}$. The samples for TEM analysis were stained with I_2.

Similarly, well-defined organic/inorganic hybrid nanofibers with a diameter of ca. 50 nm by dispersing $PTEPM_{37}$-*b*-$P2VP_{540}$ (Figure 4B (right)) were obtained, which was inherited from their bulk structure. The length of fibers reaches several micrometers, and the fiber looks semiflexible. Also, hybrid nanospheres (Figure 4C (right)) were obtained by dispersing $PTEPM_{35}$-*b*-$P2VP_{1360}$. These samples for TEM analysis had not been stained, and therefore, the dark areas in these TEM images correspond to the gelated PTEPM domains. Thus, a series of well-defined hybrid nanoobjects have been obtained. Since the P2VP hairs are densely grafted from their surfaces, the functions of these nanohybrids were explored.

Shown in Figure 5A is the appearance of the hybrid plates of $PTEPM_{58}$-*b*-$P2VP_{474}$ dispersed in water, where the pH value of the solution was changed to 9. Compared with Figure 4A (left), the sediments appeared at the bottom of the bottle and the upper solution turned clear, which means that the hybrid nanoplates precipitated from basic water. When the pH was changed back to 3, the plates were dispersed again after stirring ca. 1 day (Figure 5B). Figure S3 (in Supporting Information) showed the TEM photographs of the isolated hybrid plates after this cycle, indicating that the well-defined hybrid plates were obtained again. Similar results were obtained for the hybrid cylinders and spheres. Therefore, the isolated organic/inorganic hybrid nanoobjects not only with controlled shapes but also with pH-responsive character have been prepared by the self-assembly of novel functional gelable PTEPM-*b*-P2VP diblock copolymers.

4. Preparation of pH-Responsive Organic−Inorganic Hybrid Nanoobjects Loaded with Gold Nanoparticles. Another important property of P2VP is its coordinating ability to transition metal ions. This character makes that the obtained hybrid nanoobjects bearing P2VP hairs with different shapes can be used as the templates for stabilizing and organizing metal nanoparticles on their surface, where the P2VP hairs acted not only as dispersants for nanoobjects but also as coordinating agents of metal nanoparticles. Herein, we tried to stabilize gold nanoparticles to demonstrate this concept. To make the isolated

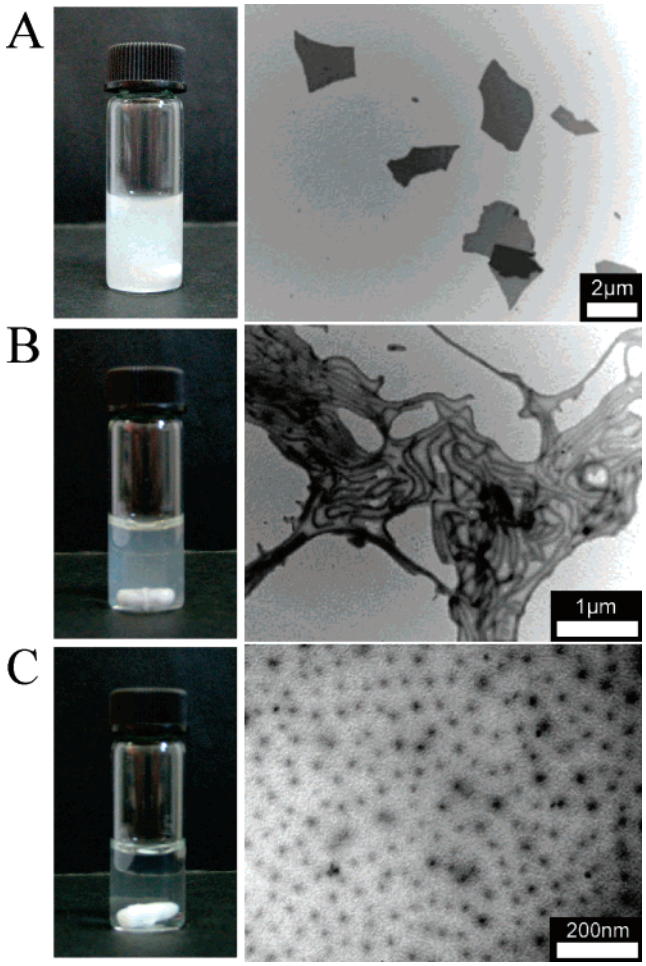

Figure 4. Photographs of dispersions (shown on left) and TEM micrographs of the hybrid nanoobjects (shown on right) obtained through dispersing the gelated bulk samples in water (pH = 3). (A) $PTEPM_{58}$-*b*-$P2VP_{474}$, (B) $PTEPM_{37}$-*b*-$P2VP_{540}$, and (C) $PTEPM_{35}$-*b*-$P2VP_{1360}$.

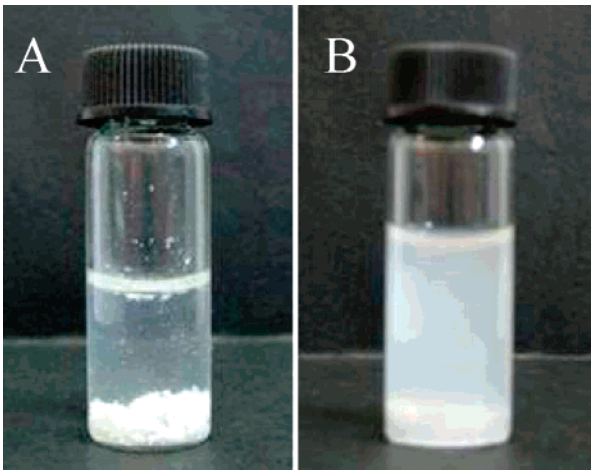

Figure 5. Photographs of the pH-responsive nanoplates dispersed in water formed by $PTEPM_{58}$-*b*-$P2VP_{474}$: (A) pH = 9 and (B) pH = 3.

nanoobjects loaded with gold nanoparticles, an important factor is the molar ratio between $NaAuCl_4$ and 2VP. If the feed ratio is too high, the metal ions may cross-link different nanoobjects and the dispersion of these nanoobjects is influenced. Here, we fixed the feed ratio between 2VP and $NaAuCl_4$ to 1:0.2.

A water solution of $NaAuCl_4$ (ca. 1 mg/mL) was added slowly into the nanoobjects with different shapes dispersed in acidic

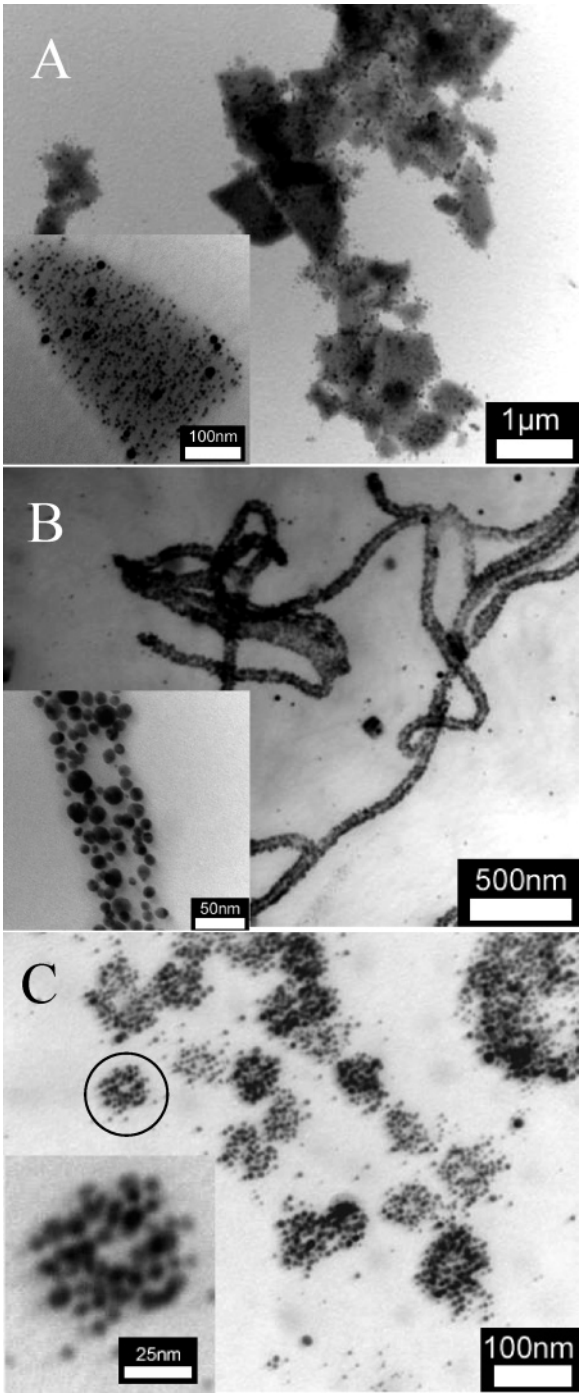

Figure 6. TEM micrographs of the hybrid nanoobjects loaded with gold nanoparticles dispersed in water (pH = 3). (A) $PTEPM_{58}$-*b*-$P2VP_{474}$, (B) $PTEPM_{37}$-*b*-$P2VP_{540}$, and (C) $PTEPM_{35}$-*b*-$P2VP_{1360}$; the circled area is one sphere bearing many gold nanoparticles, and the inset is its magnification.

water with vigorously stirring, where the molar ratio between 2VP and $NaAuCl_4$ was 1:0.2. The color of the white translucent dispersion turned pale yellow, indicating that the Au ions had been captured by the nanoobjects. After the mixture solution was stirred ca. 24 h, a freshly prepared aqueous solution of sodium borohydride (10 mg/mL) (ca. 0.1 mL) was added. The color of the solution immediately turned from pale yellow to deep red, demonstrating the formation of small Au nanoclusters.

Figure 6 includes the TEM micrographs of the isolated nanoobjects with different shapes loaded with gold nanoparticles on their surface. They clearly show that the gold nanoparticles were organized along the surfaces of three hybrid nanoobjects.

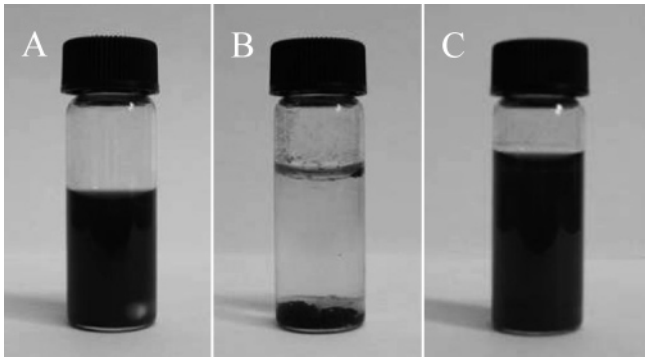

Figure 7. Photographs of the pH-responsive nanocylinders with Au nanoparticles dispersed in water: (A) pH = 3, (B) pH = 9, and (C) pH = 3.

When the plates were used, novel functional plates were obtained, where the continuous middle layer is silicon oxide network and the isolated gold nanoparticles are loaded on the two-dimensional surface of both sides (Figure 6A). Similarly, the hybrid nanocylinders with a continuous hybrid core loaded with gold nanoparticles were prepared when the cylinders were used as templates. Figure 6B shows the representative image of these novel nanocylinders, where the gold nanoparticles are aligned along one-dimension. Figure 6C is the micrograph of nanospheres loaded with gold nanoparticles formed by the hybrid spheres, where the circled area is a sphere with a diameter of ca. 60 nm bearing many Au particles. The hybrid cores cannot be observed because of the much higher electron density of gold nanoparticles. Therefore, the present nanohybrids can be an efficient platform to organize the inorganic nanoparticles into different dimensions.

These nanoobjects with gold nanoparticles also displayed pH-responsive ability. Figure 7A is the appearance of the nanocylinders loaded with gold nanoparticles on their surface formed by $PTEPM_{37}$-*b*-$P2VP_{540}$, where a dark dispersed solution was observed. When the pH of the solution was changed to 9, the sediments appeared at the bottom of the bottle and the upper solution became clear (Figure 7B). When the pH of the solution changed back to 3 with stirring for 1 day, the solution became homogeneous again (Figure 7C). The TEM image of the nanocylinders bearing gold nanoparticles after this cycle was shown in Figure S4 (in Supporting Information), the cylinders with aligned Au nanoparticles were obtained again. The pH-responsive experiments demonstrate the presence of many free 2VP units which can be protonated and deprotonated.

Conclusion

We have synthesized a class of functional gelable diblock copolymer, PTEPM-*b*-P2VP, by a RAFT mediated radical polymerization. The self-assembly of a series of PTEPM-*b*-P2VP copolymers in the bulk state was studied. With changing the molecular weight fraction of PTEPM block in the diblock copolymer from 25.6% to 16.3% to 6.6%, three different morphologies by microphase separation, i.e., lamella, hexagonally packed cylinders, and liquidlike spheres, were obtained. The new results are summarized as the following:

(1) An in-situ sol−gel reaction of triethoxylsilyl groups confined in the PTEPM microphase may generate the P2VP functionalized hybrid materials with ordered microphase structures.

(2) By dispersing the gelated bulk materials in acidic water solution (pH = 3), novel dispersible P2VP functionalized organic/inorganic hybrid nanoobjects of lamellar, cylindrical, and spherical shapes were prepared. Since the P2VP chains are densely linked with the gelated core, these hybrids may be considered as novel functional polymer brushes of different dimension. These well-defined hairy nanohybrids show stimulus responsive to pH change.

(3) The dispersible hybrids have been applied as the templates to support and organize inorganic nanoparticles by using P2VP hairs. The gold nanoparticles have been organized onto these well-defined nanoobjects with different dimensions and the loaded nanoobjects are also pH-sensitive. Theoretically, many other kinds of metal nanoparticles can also be supported onto these intelligent nanoobjects formed by PTEPM-*b*-P2VP, which will greatly expand the applications of these nanoobjects in different fields, such as catalysis and biomedicine, etc., which are under exploration.

Acknowledgment. Financial support from NSF China (50473056, 20534010, and 20625412) and the 973 program of MOST (G2003CB615605) is gratefully acknowledged. The authors thank Professor M. Schmidt and Dr. M. Maskos at University of Mainz for valuable discussions and supplying TEM and GPC measurements and thank Dr. M. Yang and Professor W. Wang at Nankai University for valuable discussions and SAXS measurements. K.Z. thanks the PPP project for supporting his visit in Mainz.

Supporting Information Available: Figures S1−S4. This material is available free of charge via the Internet at http://pubs.acs.org.

References and Notes

(1) Bates, F. S.; Frederickson, G. H. *Annu. Rev. Phys. Chem.* **1990**, *41*, 525.
(2) Bates, F. S. *Science* **1991**, *251*, 898.
(3) Hamley, I. W. *The Physics of Block Copolymers*; Oxford University Press: New York, 1998.
(4) Simon, P. F. W.; Ulrich, R.; Spiess, H. W.; Wiesner, U. *Chem. Mater.* **2001**, *13*, 3464.
(5) Haryono, A.; Binder, W. H. *Small* **2006**, *2*, 600.
(6) Bockstaller, M. R.; Mickiewicz, R. A.; Thomas, E. L. *Adv. Mater.* **2005**, *17*, 1331.
(7) Hamley, I. W. *Angew. Chem., Int. Ed.* **2003**, *42*, 1692.
(8) Park, M.; Harrison, C.; Chaikin, P. M.; Register, R. A.; Adamson, D. H. *Science* **1997**, *276*, 1401.
(9) Cheng, J. Y.; Ross, C. A.; Chan, V. Z. H.; Thomas, E. L.; Lammertink, R. G. H.; Vancso, G. J. *Adv. Mater.* **2001**, *13*, 1174.
(10) Liu, G. J.; Qiao, L. J.; Guo, A. *Macromolecules* **1996**, *29*, 5508.
(11) Liu, G. J.; Yan, X. H.; Duncan, S. *Macromolecules* **2002**, *35*, 9788.
(12) Ishizu, K.; Fukutomi, T. *J. Polym. Sci., Part C: Polym. Lett.* **1988**, *26*, 281.
(13) Ishizu, K. *Polym. Commun.* **1989**, *30*, 209.
(14) Yan, X. H.; Liu, F. T.; Li, Z.; Liu, G. J. *Macromolecules* **2001**, *34*, 9112.
(15) Saito, R.; Fujita, A.; Ichimura, A.; Ishizu, K. *J. Polym. Sci., Part A: Polym. Chem.* **2000**, *38*, 2091.
(16) Erhardt, R.; Boker, A.; Zettl, H.; Kaya, H.; Pyckhout-Hintzen, W.; Krausch, G.; Abetz, V.; Müller, A. H. E. *Macromolecules* **2001**, *34*, 1069.
(17) Zheng, R. H.; Liu, G. J.; Yan, X. H. *J. Am. Chem. Soc.* **2005**, *127*, 15358.
(18) Yan, X. H.; Liu, G. J.; Liu, F. T.; Tang, B. Z.; Peng, H.; Pakhomov, A. B.; Wong, C. Y. *Angew. Chem., Int. Ed.* **2001**, *40*, 3593.
(19) Yan, X. H.; Liu, G. J.; Li, Z. *J. Am. Chem. Soc.* **2004**, *126*, 10059.
(20) Liu, G. J.; Ding, J. F. *Adv. Mater.* **1998**, *10*, 69.
(21) Liu, G. J.; Ding, J. F.; Hashimoto, T.; Kimishima, K.; Winnik, F. M.; Nigam, S. *Chem. Mater.* **1999**, *11*, 2233.
(22) Templin, M.; Franck, A.; DuChesne, A.; Leist, H.; Zhang, Y. M.; Ulrich, R.; Schadler, V.; Wiesner, U. *Science* **1997**, *278*, 1795.
(23) Ulrich, R.; Du Chesne, A.; Templin, M.; Wiesner, U. *Adv. Mater.* **1999**, *11*, 141.
(24) Finnefrock, A. C.; Ulrich, R.; Du Chesne, A.; Honeker, C. C.; Schumacher, K.; Unger, K. K.; Gruner, S. M.; Wiesner, U. *Angew. Chem., Int. Ed.* **2001**, *40*, 1207.

(25) Garcia, C. B. W.; Zhang, Y. M.; Mahajan, S.; DiSalvo, F.; Wiesner, U. *J. Am. Chem. Soc.* **2003**, *125*, 13310.
(26) Garcia, C.; Zhang, Y. M.; DiSalvo, F.; Wiesner, U. *Angew. Chem., Int. Ed.* **2003**, *42*, 1526.
(27) Jain, A.; Toombes, G. E. S.; Hall, L. M.; Mahajan, S.; Garcia, C. B. W.; Probst, W.; Gruner, S. M.; Wiesner, U. *Angew. Chem., Int. Ed.* **2005**, *44*, 1226.
(28) Zhang, K.; Gao, L.; Chen, Y. M. *Macromolecules* **2007**, *40*, 5916.
(29) Lazzari, M.; López-Quintela, M. A. *Adv. Mater.* **2003**, *15*, 1583.
(30) Ozaki, H.; Hirao, A.; Nakahama, S. *Macromolecules* **1992**, *25*, 1391.
(31) Alberti, A.; Benaglia, M.; Laus, M.; Sparnacci, K. *J. Org. Chem.* **2002**, *67*, 7911.

MA7021698